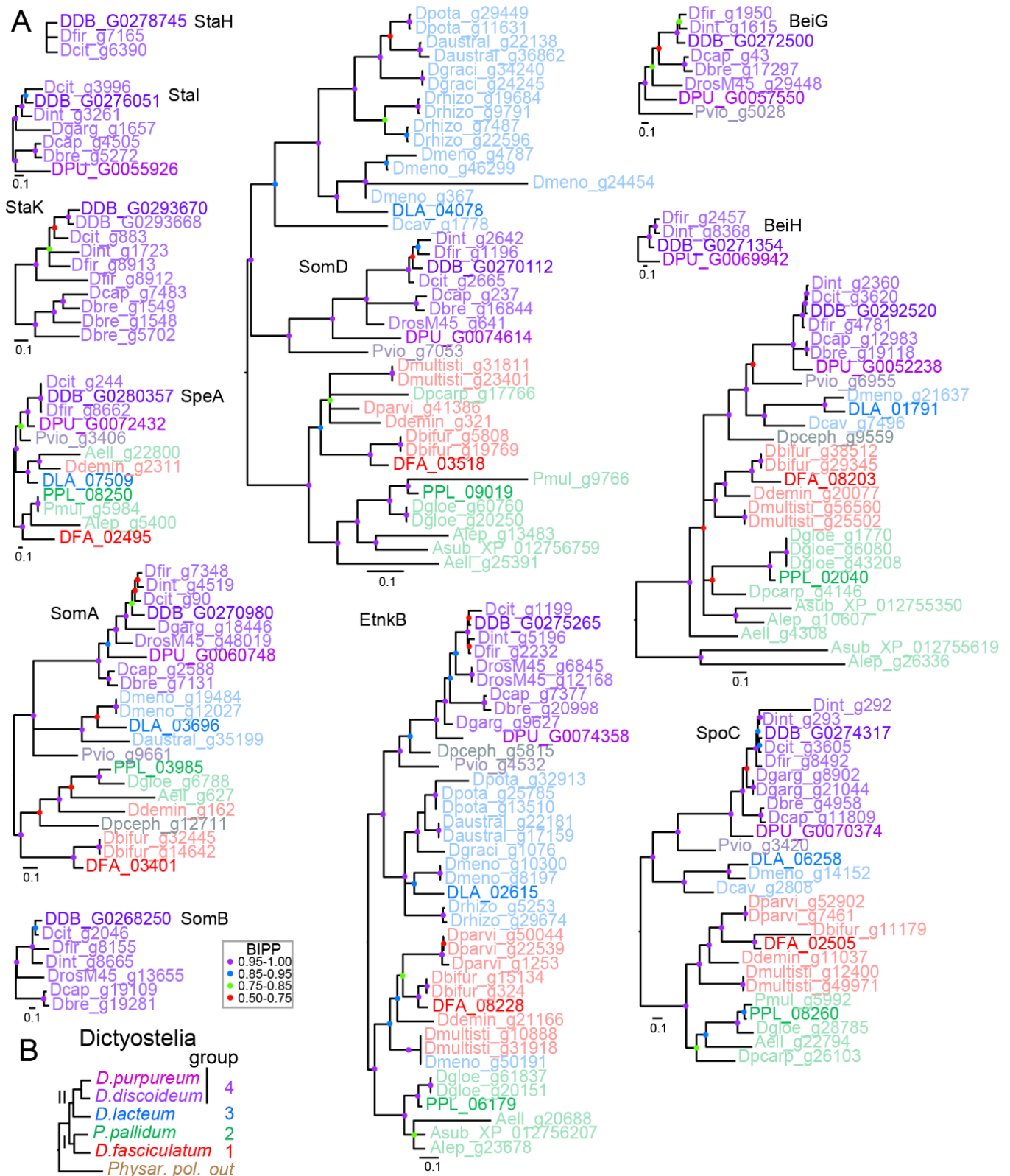


## Supplementary Figures S1-S7 and supplementary Table S1

**Figure S1. Evolutionary conservation of newly analysed cell type marker genes**

**A. Gene conservation.** For the cell type marker genes that were analysed in figure 1, closest relatives were identified by BLASTp in a protein sequence library compiled from 47 annotated genomes and transcriptomes, representative of all major and minor taxon groups of Dictyostelia. The locus tags of the genes are colour coded according to the taxon group to which the host species belongs (B) with the more intense colours representing the well annotated *D. discoideum*, *D. purpureum*, *D. lacteum*, *P. pallidum* and *D. fasciculatum* genomes. Species belonging to minor taxon groups are colour coded in grey. Protein sequences were aligned

with Clustal Omega (Sievers and Higgins, 2014) with five combined iterations and phylogenies were inferred using MrBayes 3.2 (Ronquist and Huelsenbeck, 2003). Posterior probabilities (BIPP) of the nodes are indicated by coloured dots. Full species names and Bioproject or Assembly IDs of the genomes and transcriptomes that were used are listed in SupData1\_Genes&Species.xlsx.

*B. Dictyostelid phylogeny.* Phylogeny of the five taxon-group-representative *Dictyostelium* species for which developmental- and cell type specific transcriptome data are shown in Figure 1B. The phylogeny was inferred from 30 concatenated proteins and rooted on the non-dictyostelid Amoebozoan *Physarum polycephalum* (Romeralo et al., 2013).

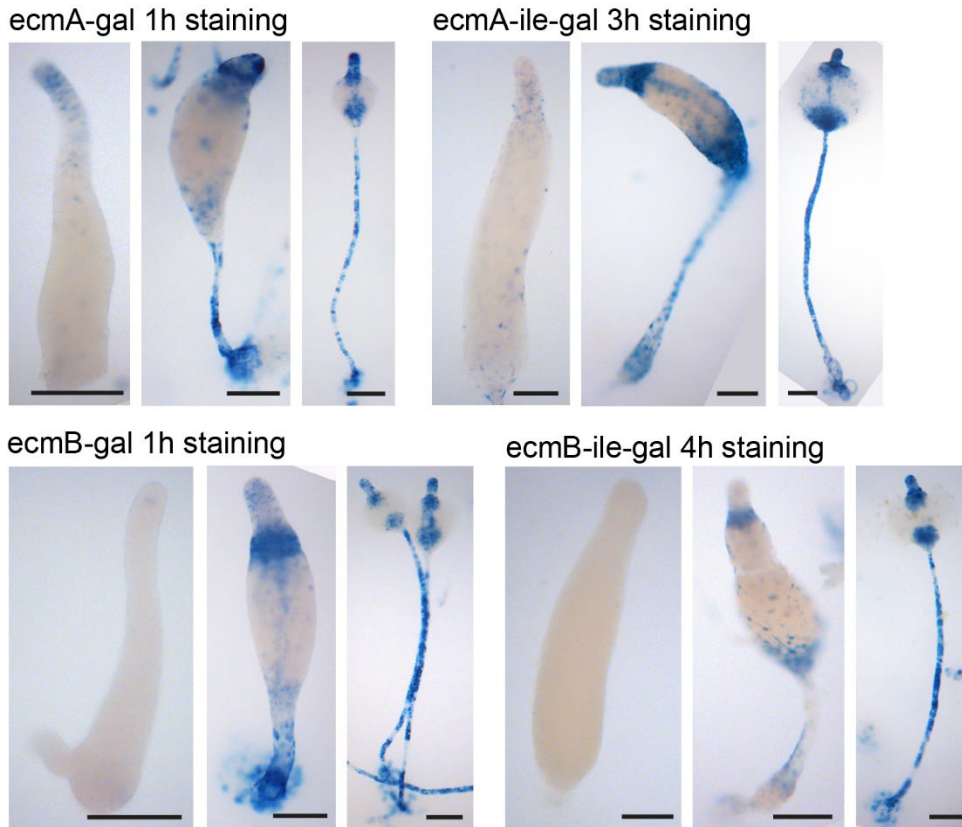


**Figure S2. Standardized staining of cells transformed with *ecmA*- and *ecmB*-*lacZ***

*Ax2* cells transformed with *ecmA-lacZ*, *ecmA-ile-lacZ*, *ecmB-lacZ* and *ecmB-ile-lacZ* (Detterbeck et al., 1994; Jermyn and Williams, 1991) were incubated on nitrocellulose filters supported by non-nutrient agar until migrating slugs, mid-culminants and fruiting bodies were formed. After fixation, the structures were stained with X-gal for the period required to strongly but not overstain the culminants and fruiting bodies. Bar: 100  $\mu$ m. Note that the poor expression in slugs is not a consequence of  $\beta$ -galactosidase accumulating in the later stages, since the unstable ile-gal forms (Detterbeck et al., 1994) also show poor staining in slugs compared to fruiting bodies.



**B. Transcriptomics.** The developmental time courses and cell type specificity data of the markers were retrieved from published RNAseq experiments as described in the legend to Figure 1. When known, gene names are also listed. Identifiers in grey text represent genes not otherwise used in this study.

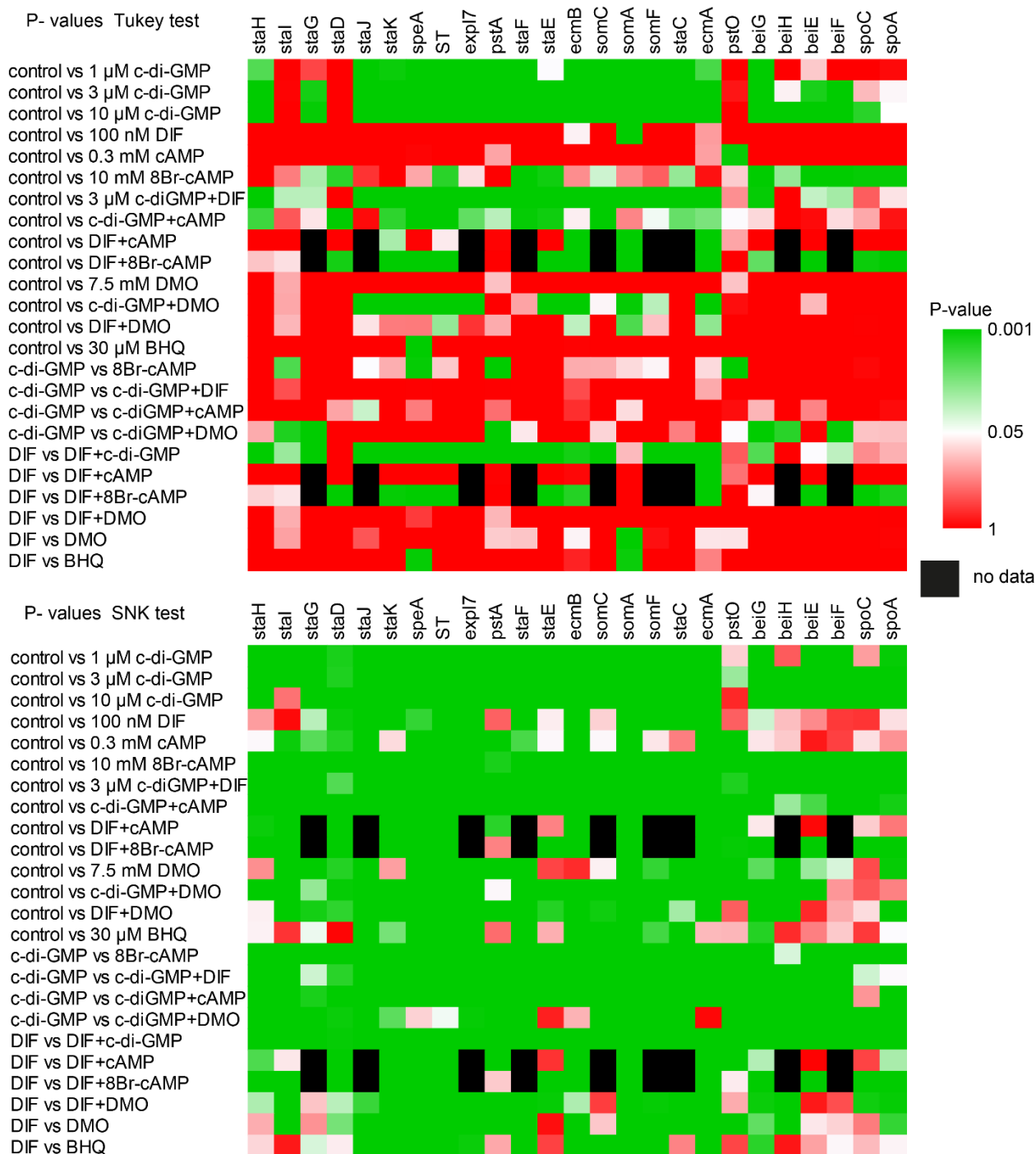


**Figure S4. P-values for pair-wise comparison of the differential effects of stimuli on gene induction**

The data describing the effects of 15 stimulation regimens on 25 genes that are presented in figure 2 were subjected to Kruskal-Wallis ANOVA on ranks to identify significant differences between treatments on each of the genes. The stringent Tukey test and less stringent Student-Newman-Keuls (SNK) test were used to calculate P-values for the null hypothesis of no difference between treatments. The full analysis of 105 pairwise comparisons is listed with the experimental data for each gene in SupData2\_Induction.xlsx. Biologically relevant comparisons are shown here as heatmaps of the P-values obtained with either test. Black squares represent experiments that were only performed once or not at all. Combined treatments used 3  $\mu$ M c-di-GMP and the same concentrations for the other compounds as used for single treatments.

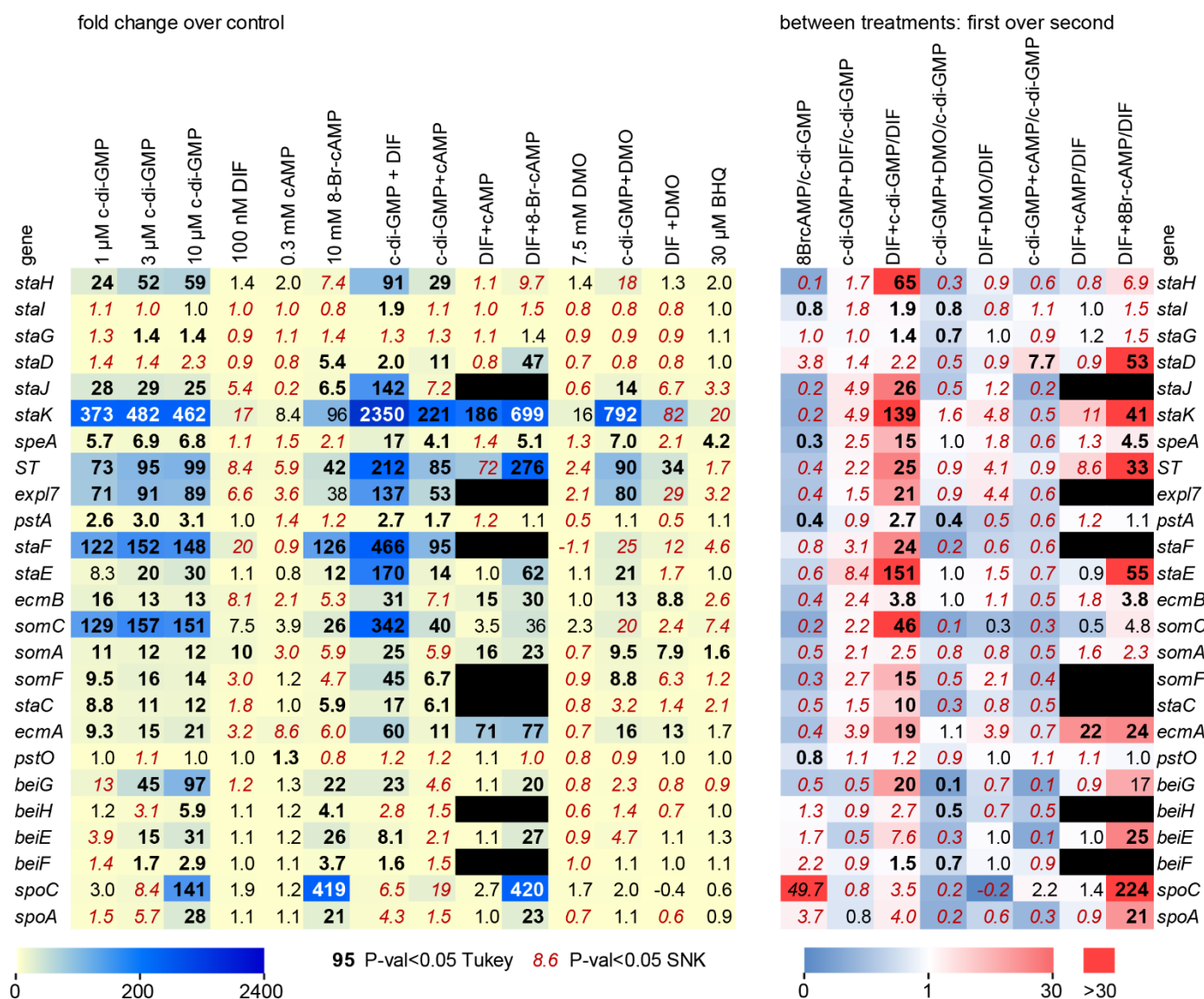


**Figure S5. Fold-change differences between treatments annotated with P-values**

The table lists the numerical values of the fold-change over control values (left panel) and fold-changes between different treatments (right panel). The values are presented in different fonts to reflect whether the difference between treatments is significant ( $P < 0.05$ ) as assessed by ANOVA on ranks with P-values calculated by either the stringent Tukey test (bold black or white font) or the less stringent SNK test (italic red font). The extent of fold-change is further indicated as a yellow-blue heatmap in the left panel and a blue to red heatmap in the right panel, where a blue background marks a reduced effect and a red background an increased effect of the first over the second treatment, shown at the top of each column. Black boxes represent absent data. Note that small fold-changes can be statistically significant when there is little variation between individual experiments, while large fold-changes may not reach significance because the absolute value of the change varies strongly between experiments. We therefore also show the data and their analysis in `Supdata2_induction.xlsx`.

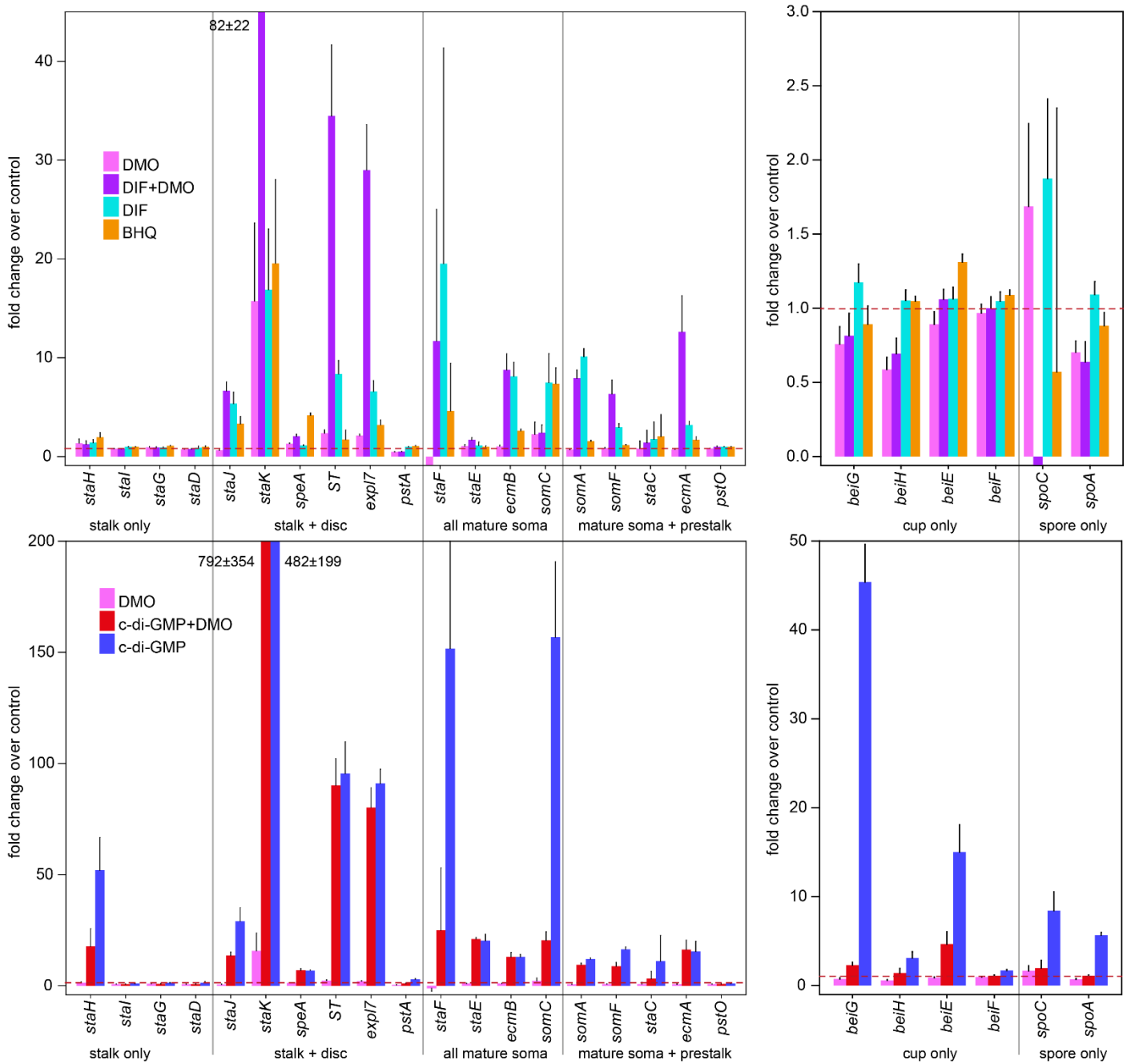


**Figure S6. Gene induction expressed as fold-change of control**

For a subset of the gene induction data presented in Figure 2 where relatively small effects of stimuli were observed, data are re-plotted here as means and SE of fold-change over control (no addition). The red dashed line marks the control value of 1.

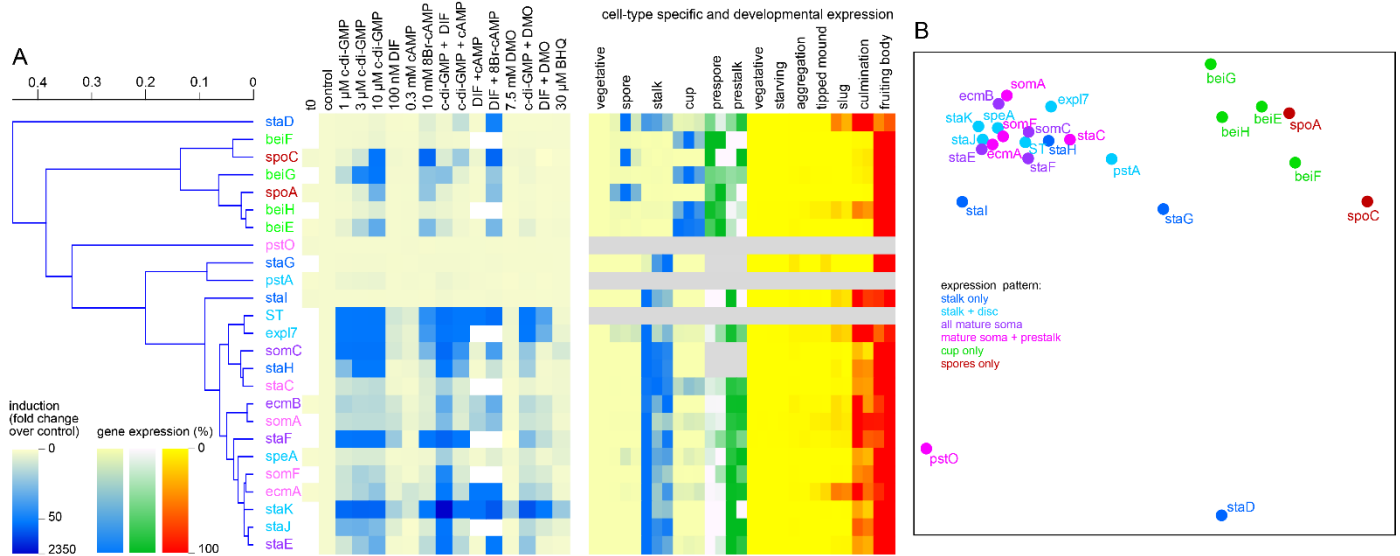


**Figure S7. Hierarchical clustering of gene induction data relative to fold change**

*A. Hierarchical tree.* The averaged data for induction of 25 genes by 15 single or combined stimuli as presented in figure 2 are expressed here as fold-change relative to control and subjected to hierarchical clustering as described for figure 3. The hierarchical tree is combined with a heatmap of the gene induction responses as fold-change over control and a heatmap of the cell-type specific and developmental expression of the genes.

*B. Multidimensional scaling.* The induction data relative to fold-change were also used to cluster the genes by multidimensional scaling as in figure 3.



- Jermyn, K. A., Berks, M., Kay, R. R. and Williams, J. G.** (1987). Two distinct classes of prestalk-enriched mRNA sequences in *Dictyostelium discoideum*. *Development* **100**, 745-755.
- Jermyn, K. A. and Williams, J. G.** (1991). An analysis of culmination in *Dictyostelium* using prestalk and stalk-specific cell autonomous markers. *Development* **111**, 779-787.
- Kin, K., Forbes, G., Cassidy, A. and Schaap, P.** (2018). Cell-type specific RNA-Seq reveals novel roles and regulatory programs for terminally differentiated *Dictyostelium* cells. *BMC Genomics* **19**, 764.
- Romeralo, M., Skiba, A., Gonzalez-Voyer, A., Schilde, C., Lawal, H., Kedziora, S., Cavender, J. C., Glockner, G., Urushihara, H. and Schaap, P.** (2013). Analysis of phenotypic evolution in *Dictyostelia* highlights developmental plasticity as a likely consequence of colonial multicellularity. *Proc Biol Sci* **280**, 20130976.
- Ronquist, F. and Huelsenbeck, J. P.** (2003). MrBayes 3: Bayesian phylogenetic inference under mixed models. *Bioinformatics* **19**, 1572-1574.
- Sievers, F. and Higgins, D. G.** (2014). Clustal omega, accurate alignment of very large numbers of sequences. *Methods in molecular biology* **1079**, 105-116.